Power System Protection and Control
ISSN:1674-3415

DATA FUSION AND STABILITY ANALYSIS WITH ALPHA FAMILY METHOD APPROXIMATION ESTIMATORS FOR SATELLITE ORBIT DETERMINATION

Nisha S.L.[1], Dr. B.K. Sujatha[2], Dr. J.R. Raol[3]

[1]Assistant Professor, Department of ETE, Ramaiah Institute of Technology (RIT), Bangalore and Doctoral Research Student, Visvesvaraya Technological University (VTU). Email: nisha_sln@msrit.edu
[2]Research Guide, Department of ETE, Ramaiah Institute of Technology (RIT), Bangalore. Email: bksujatha@msrit.edu
[3]Independent Consultant - Estimation & Control, Former Sr. Scientist & Head, FMCD, NAL-CSIR, & Emeritus Professor, Department E&C, M.S. Ramaiah Institute of Technology (MSRIT), Bangalore. Email: raoljr@gmail.com

Received: 29/03/2026 **Revised**: 24/04/2026 **Accepted**: 27/05/2026

***ABSTRACT*:**

Accurate and robust satellite orbit determination is essential for space missions, navigation, and remote sensing. This paper presents a comparative analysis of three nonlinear state estimation techniques like Extended Kalman Filter (EKF), Particle Filter (PF), and the Alpha Filter (AF) focusing on their performance in estimating satellite position and velocity under noisy conditions. A simulated orbit scenario for Low earth orbit (LEO) is used, with Gaussian noise added to sensor measurements to introduce real-world uncertainties. Here, the Satellite orbit-determination (OD) process is described and presents the results of numerical simulation of Satellite orbit estimation using Alpha Family Method Approximation estimators (AFMAE's). Additionally, a proposed observer for a nonlinear continuous time dynamic system makes use of the corresponding matrix Riccati type differential equation and gain from the theories of the AFMAE. Then, the condition for the local asymptotic stability for the error dynamics of the observer is derived using the Lyapunov energy (LE) functional. AFMAE-based sensor data fusion methodology is introduced. A data fusion scheme that utilizes the AFMAE's for unified state model (U7) and inertial coordinate set (IC6) orbital trajectories is presented in state vector level fusion (SVF). State vector level Data fusion is illustrated by implementing two AFME's. All the filtering schemes and data fusion algorithms have been validated using simulated data generated in MATLAB.

***Keywords**: Satellite orbit determination, Alpha Family Method Approximation estimators, sensor data fusion, nonlinear observer, Lyapunov energy functional and state vector level fusion.*

INTRODUCTION

Non-linear filtering is a computational tool that is extensively needed to estimate the states of a stochastic dynamic-system. The vast applications of non-linear filtering include Aircraft parameter estimation, Satellite Orbit Determination, object tracking, weather prediction, process control and so on. Kalman filter provides an optimal solution for a system linear with additive Gaussian noise assumption. However, there is no analytical solution for non-linear systems as the underlying Bayesian integrals are very complicated to solve. In this scenario, appropriate approximations are required to obtain a suboptimal solution. Suboptimal solutions are associated with a possibility of improvement. State estimation involves predicting the internal state of a dynamic-system (e.g., position and velocity of a satellite) based on noisy measurements and possibly uncertain dynamics. The goal is to estimate the system true states accurately as possible given the available information. [1-10]

DOI: 10.46121/pspc.54.2.41

Power System Protection and Control
ISSN:1674-3415

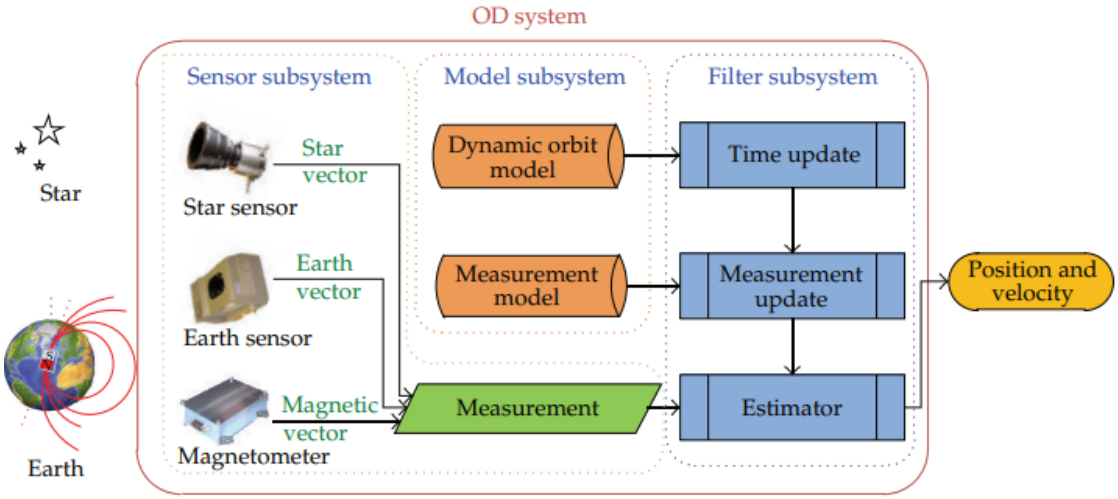

Fig. 1. Orbit Determination Process [1]

Fig. 2.

Orbit determination (OD), which aims to accurately estimate a satellite's ephemeris at a chosen epoch, is essential to satellite missions. For non-linear systems, like the non-linear dynamic model of satellite-orbit motion, the filtering method employed in the OD-system is appropriate. As shown in Figure 1, an orbit determination system normally consists of a filter subsystem, model subsystem, and sensor subsystem. To measure and process the initial measurements, which are functions of state variables, the sensor subsystem includes sensing devices such a magnetometer, earth sensor, and star sensor. State and measurement models are among the estimated data produced by the model system. The best algorithms for filtering methods in the filter subsystem process data from the model and sensor subsystems before estimating state variables. [11-20]

Three primary techniques are employed in satellite OD systems: extended Kalman filter (EKF), unscented Kalman filter (UKF), and unscented particle filter (UPF). The Taylor-series analytical expansion of the measurement equations and non-linear systems serves as the foundation for the EKF. It operates on the premise that a Gaussian random variable approximates the state distribution. However, because of the ignored nonlinearities, the Taylor-series approximations in EKF create significant inaccuracies. The UKF has the drawback of not being applicable to general non-Gaussian distributions. It does this by using the real non-linear model and a collection of sigma sample points generated by the unscented -transformation to represent the covariance and mean of the state. A flexible and principled method for estimating nonlinear states in uncertain situations is the Alpha Filter. Satellite navigation, orbit prediction, and other aerospace applications involving multiple sensor fusion and unpredictable dynamics are particularly well-suited for its ability to seamlessly transition between optimality and robustness. A member of the α-family of nonlinear estimators, the Alpha Filter, also known as the Alpha Estimator, generalizes and combines different filtering techniques using a configurable parameter $\alpha \in [0,1]$. Because of its ability to operate in uncertain, nonlinear, and possibly non-Gaussian systems, it is very helpful in intricate applications such as determining the orbit of satellites. [21-30].

The AFMAE is a versatile and robust method used in the field of state estimation for dynamic systems. It is particularly valuable in scenarios where the systems are nonlinear, and the noise involved is non-Gaussian or where traditional linear filters like the Kalman Filter may not perform optimally. The Alpha Family Approximation Estimator is a generalization of several estimation techniques, offering a range of methods depending on the parameter alpha α chosen. The parameter-α controls the balance between the prediction from the system model and the correction based on new measurements.

ALPHA FAMILY METHOD APPROXIMATION (AFMA)

A known characteristic function (CF) that is dependent on a limited number of unknown parameters is used in the AFMA in place of the unknown CF. A series of equations are then constructed and solved for the unknown parameters using the provided equation for the CF. The steps are as follows:

- $\varphi_k(\lambda, \mu)$ is replaced by the function $\varphi_k(\lambda, \mu, \alpha_k)$.

DOI: 10.46121/pspc.54.2.41

- The pdf $p_k(x, \tilde{x})$ is replaced by $p_{k-1}(x, \tilde{x}, \alpha_{k-1})$ that is required to assess the expectation but is not explicitly stated in the CF equation.
- Derivation for representing the moments of the random vector $[x^T(k)\tilde{x}^T(k)]^T$ and after differentiating with respect to λ and μ. Then the resulting equation is substituted at λ = 0 and μ = 0.
- Since the alpha family is the basis for these moments, the difference in equation in the sequence of α_k can be obtained.
- The necessary moments for estimating a recursive form are obtained by representing α_k by the moments set of the vector $[x^T(k)\tilde{x}^T(k)]^T$ up to a given order.

The differential/difference equation (DDE) for the moments will typically be unbounded. In engineering practice, knowing only the first two moments of the distributions is sufficient. The selection of this pdf also affects correctness, and the alpha family parameters dimensions must match the moments total number, that describes the pdf. For a particular class of control issues, this PDF is assumed to be Gaussian. [[9] [10]

Let the dynamic model of the system be as follows:

$$\dot{x}(t) = f(x,t) + g(x,t)\, v(t) \quad (1)$$

$$z(t) = h(x,t) + q(x,t)\, v(t) \quad (2)$$

The Ito Stochastic differential equation (ISDE)

$$dx(t) = f(x,t)\, dt + g(x,t)\, d\beta(t) \qquad t \geq t_0 \quad (3)$$

$$dz(t) = h(x,t)\, dt + q(x,t)\, d\eta(t)$$

(4)

x(t) is the state vector, which includes position and velocity.
$f(x,t)$ is the deterministic part of the state transition.
$g(x,t)$ is the process noise matrix.
v(t) is the process noise.
z(t) is the measurement vector.
$h(x,t)$ is the measurement function.
$q(x,t)$ is the measurement noise matrix.
w(t) is the measurement noise.
The estimator/estimation belongs to the class of allowable estimates as defined by [1]

$$\hat{x}(t) = Cy(t) \quad (5)$$

$$dy = G\xi(y,z,t)dt + K\zeta(y,z,t)dz + bdt \quad (6)$$

In (5), and (6) we have:
a) 'C' as a constant matrix of suitable dimensions, the estimate of x can be expressed as a linear function of y.
b) G, K are the gain matrices of suitable dimensions;
c) $\xi(.)$ is the pre-assignable vector valued function
d) $\zeta(.)$is the pre-assignable matrix valued function; and
e) 'b' is the gain vector. The latter can be regarded as the bias vector that is also unknown and gets estimated along with the filter solution. The functions in (4) determine the structure of the Pugachev's nonlinear estimator along with the proper choice of the constant matrix C. By applying the mean square error (MSE) minimization criterion, the time-dependent gains G, K, and 'b' are determined using the following formulas: [11]

$$CG = (m_{01} - CKm_{21})m_{11}^{-1}$$

$$CK = m_{02}\, m_{22}^{-1}$$

$$Cb = E_0 - CGE_1 - CKE_2 \quad (7)$$

with

DOI: 10.46121/pspc.54.2.41

$$m_{01} = E\{(f - E_0)\xi^T\}$$
$$m_{12} = m_{21}^T = E\{(\xi - E_1)h^T\zeta^T\}$$
$$m_{11} = E\{(\xi - E_1)\xi^T\}$$
$$m_{02} = E\{(x - Cy)h^T\zeta^T\} + E\{gQq^T\zeta^T\}$$
$$m_{22} = E\{\zeta qQq^T\zeta^T\}$$
$$E_0 = E\{f(x,z,t)\}$$
$$E_1 = E\{\xi(y,z,t)\}$$
$$E_2 = E\{\zeta(y,z,t)h(x,z,t)\} \quad (8)$$

The first two moments for the system generated by a non-linear function, such as f(x,t), is divided into its constituent parts using the alpha family technique, which yields the following equations:

$$\dot{m}_x = F_d + Am_x + E[f_{NL}] \quad (9)$$
$$\dot{P} = (A+B)P + P^T(A+B)^T + F + F^T + Q \quad (10)$$

Where m_x = Expectation of x, E{x}
F_d = Determinate function independent of $(x-m_x)$
A = State x's linear function
B = Linear function in $(x-m_x)$
P = Correlation movement matrix
R=measurement noise covariance matrix
$F = E\{f_{NL}(x-m_x))^T\}$
f_{NL} = Nonlinear components of f
Q = The variance (or intensity) associated with the noise process w(t)

Time updates

Computation of the gains is based on the one-dimensional joint characteristic function φ(.). The vector processes x, z, and y is given as joint characteristic function

$$\emptyset_k(\lambda, \mu, \alpha) = E\{\exp(i\lambda^T x(k) + i\mu^T \hat{x}(k) + i\,\alpha_0^T z(k))\} \quad (11)$$
$$\emptyset_k(\lambda, t) = E\{\exp(i\lambda^T x(t))\} \quad (12)$$
$$\frac{\partial \emptyset_k(\lambda,t)}{\partial t} = E\{\exp(i\lambda^T f(x,t) + \psi(\lambda,x,t))\} \quad (13)$$

Where $\psi(\lambda, x, t)$ partial derivative value of the characteristic function.
$\emptyset_k(\lambda, \mu, \alpha)$of the random process

$$w_1 = \int_t^s g(x(\tau),\tau)w(\tau)d\tau \quad (14)$$
$$\psi(\lambda, x, t) = \frac{\partial \emptyset_k(\lambda,x,t,s)}{\partial t} \quad \text{for s=t} \quad (15)$$

Measurement update

$$\hat{x}^+(t+1) = \alpha\xi + \beta\zeta z + \gamma \quad (16)$$

Where $\alpha, \beta and\ \gamma$ are optimal gains
Next, applying the notion of MS error estimation

$$E\{(x(t+1) - E\{x(t+1)\})(\xi^T z^T \zeta^T)\} = [\alpha\beta]E\left\{\begin{bmatrix}\xi - E(\xi)\\ \zeta z - E(\zeta z)\end{bmatrix}[\xi^T \quad z^T \quad \zeta^T]\right\} \quad (17)$$
$$\gamma = E\{x(t+1)\} - [\alpha\beta]\begin{bmatrix}E(\xi)\\ E(\zeta z)\end{bmatrix} \quad (18)$$

Intermediate gains

$$[k_{01} \quad k_{02}] = [\alpha\beta]\begin{bmatrix}k_{11} & k_{12}\\ k_{21} & k_{22}\end{bmatrix} \quad (19)$$

DOI: 10.46121/pspc.54.2.41

Power System Protection and Control
ISSN:1674-3415

LYAPUNOV STABILITY ANALYSIS FOR THE ALPHA FAMILY METHOD APPROXIMATION ESTIMATOR

For the system of (1) a nonlinear observer is given as,

$$\hat{x}(t_{k+1}) = \hat{x}(t_k) + \alpha\Delta t[f(\hat{x}(t_k), t_k) + L(z(t_k) - h(\hat{x}(t_k), t_k)) \quad (20)$$

$$\hat{z}(t_k) = h(\hat{x}(t_k), t_k) + q(x(t_k), t_k)v(t_k) \quad (21)$$

The state estimate is updated at discrete time steps t_k according to equation (16) by the AFMA estimator:
Define the estimation error as:

$$e(t_k) = x(t_k) - \hat{x}(t_k) \quad (22)$$

$$e(t_{k+1}) = e(t_k) + \alpha\Delta t[f(x(t_k), t_k) - f(\hat{x}(t_k), t_k) + \Delta t g(x(t_k), t_k)v(t_k) - L\big(h(x(t_k), t_k) - h(\hat{x}(t_k), t_k)\big) + q(x(t_k), t_k)v(t_k) \quad (23)$$

Gain of the filter $L = PHR^{-1}$ (24)

The linearization of the system dynamics is:

$$f(x(t_k), t_k) \approx f(\hat{x}(t_k), t_k) + A(t_k)\, e(t_k) \quad (25)$$

$$h(x(t_k), t_k) \approx h(\hat{x}(t_k), t_k) + B(t_k)\, e(t_k) \quad (26)$$

where

$A(t_k) = \left.\frac{\partial f}{\partial x}\right|_{\hat{x}(t_k), t_k}$ is the system dynamics Jacobian matrix. (27)

$B(t_k) = \left.\frac{\partial h}{\partial x}\right|_{\hat{x}(t_k), t_k}$ is the measurement function Jacobian matrix. (28)

Substituting these into the error dynamics yields:

$$e(t_{k+1}) = (I - \alpha\Delta t A(t_k) - LB(t_k))e(t_k) + \Delta t g(x(t_k), t_k)v(t_k) + q(x(t_k), t_k)v(t_k) \quad (29)$$

To determine the convergence condition of the observer error equation (29) Lyapunov-Krasovskii's approach is used, for which the following equations are used:
In general, the error state is denoted as:

$$e(t+1) = G\, e(t) \quad (30)$$

The Lyapunov energy function (LEF) be defined as

$$V(e(t)) = (e^T(t))\, Y(t)\, e(t)) \quad (31)$$

Y(.) in (25) is a positive definite matrix for the information matrix (the inverse covariance matrix of P) and uses the derivative of the LEF in the following expression:

$$\Delta\{V(e(t))\} = V(e(t+1)) - V(e(t)) \quad (32)$$

The observer error dynamics convergence is determined, using the LEF (continuous time domain) time derivative and searching for circumstances that make this time derivative negative definite, the comparable convergence analysis is performed in the continuous time case.as shown in (29).
Substituting for V(.)s' in (26) to obtain

$$\begin{aligned} \Delta\{v(e(t))\} &= V(e(t+1)) - V(e(t)) \\ &= e^T(t+1)Ye(t+1) - e^T(t)ye(t) \\ &= e^T(t)G^TYGe(t) - e^T(t)ye(t) \\ &= e^T(t)[G^TYGe(t) - Y]e(t) \end{aligned} \quad (33)$$

The observer error dynamics convergence requires the "derivative" term of the error to be negative definite,

$$\Delta\{v(e(t))\} = -e^T(t)[-(G^TYG - Y)]\, e(t) \quad (34)$$

The condition of the observer error dynamics convergence is as follows:

$$-[G^TYG - Y] = Y - G^TYG \quad (35)$$

Equation (29) is positive definite (PD). The following condition is true for the magnitudes of the terms involved

$$|Y - G^TYG| > 0 \quad (36)$$

The matrix magnitude is measured by its norm, the final condition is

DOI: 10.46121/pspc.54.2.41

$\|Y - G^T YG\| > 0 \quad \|G^2\| < 1$ (37)

The convergence condition is derived from the observer's error dynamics of (32) is got in the form of (37) to define certain bounds as follows:

$P_l \leq P(.) \leq P_u$ is the range of the steady state solution (38)

P_u, P_l are positive numbers. The positive definite/ symmetric (PD) matrix is P(.).

The terms A, B, V, G, Q and R is bounded as

$\|A\| = s\ ; \|B\| = b; \|G\| = g\ ; \|V\| = v; \|R\| = r\ ; \|Q\| = q; \quad \|I\| = i$

(39)

The 'p' variable is a scalar factor that represents the upper bound of the related nonlinear function.

$\|P\| = p$ (40)

In order to simplify the error dynamics, the following bounds on the norms of matrices H is required:

$\|HH^T\| = h;$ and the norm of error is given by $\|e(k)\| = \varepsilon$ (41)

Eqn(23) is the observer's error dynamics derived in the form of

$\|e(t+1)\| = (i - \alpha s - \frac{phb}{r})\epsilon + gv + qv$ (42)

$\|e(t+1)\| = \|G\|\|\mathrm{e}(t)\|$ (43)

The terms in (37) is replaced by their norms as follows

$\|e(t+1)\| = [\left(\mathrm{i} - \alpha\mathrm{s} - \frac{phb}{r}\right) + (\frac{v(g+q)}{\epsilon})]\|\mathrm{e}(t)\|$ (44)

Substitute all the bounds from (42) and also simplify the resultant expression, and use the error norm definition, to obtain:

$\|e(t+1)\| = \|G\|\|\mathrm{e}(k)\|$ (45)

Compare Equations (44) and (45) to get

$\|G\| = [(i - \alpha s - \frac{phb}{r}) + (\frac{v(g+q)}{\epsilon})]$ (46)

Taking the principal (positive) square root of 1and applying the condition of (37) to get,

$\|G^2\| = [(i - \alpha s - \frac{phb}{r}) + (\frac{v(g+q)}{\epsilon})\ ]^2 < 1$ (47)

$[(i - \alpha s - \frac{phb}{r}) + (\frac{v(g+q)}{\epsilon})]\ < sqrt(1) = \pm 1$ (48)

Consequently, the observer's error dynamics convergence condition is derived as

$\frac{v(g+q)}{\epsilon} < 1 - \left(i - \alpha s - \frac{phb}{r}\right)$ (49)

In (49) all the coefficients are well defined and are the positive bounding constants in (48). The condition of (49) means that, the Lyapunov energy functional's differential in equation (34) would be negative definite, the error would (asymptotically) reach zero as the observer error dynamics converge. Since the observer error dynamics made use of the Alpha Family Method Approximation Estimator's gain and covariance matrix, this further proves that the estimator would likewise converge. This is a new method of using the deterministic observer to prove the asymptotic stability of the discrete time AFME.

DATA FUSION SCHEME WITH THE ESTIMATORS

The continuous observer's and the AFMA estimators-based data fusion scheme's performances are assessed through MATLAB simulation. The results demonstrate that the nonlinear observer behaves asymptotically and the convergence properties of data fusion scheme. This contribution has a novel feature in the form of this kind of validation study. Using the gain from the theory of AFMA, a nonlinear observer for continuous time systems is described. It also makes use of the matrix Riccati type differential (RTD) equation, which is required for the gain computation [12] .The asymptotic stability result for the observer is derived using the Lyapunov energy functional (26). The performance of the nonlinear observer is demonstrated by implementing these algorithms in MATAB.

Let the dynamic model of the system be the following:

An approximation method for nonlinear filtering is the Alpha Family Estimator. The two-state estimation can be structured as foliows:

State Prediction (One-Step Ahead):

$\hat{\mathrm{x}}^{+}(\mathrm{t_{k+1}}) = \hat{\mathrm{x}}(\mathrm{t_k}) + \alpha \mathrm{f}(\hat{\mathrm{x}}(\mathrm{t_k}), \mathrm{t_k}) + \mathrm{L}(\mathrm{z}(\mathrm{t_k}) - \mathrm{h}(\hat{\mathrm{x}}(\mathrm{t_k}), \mathrm{t_k}))$ (54)

Where Alpha α is a parameter in the Alpha Family method, typically between 0 and 1.

L is the gain matrix (analogous to the Kalman gain but derived using the Alpha Family method).

DOI: 10.46121/pspc.54.2.41

$\hat{x}(t_K)$ is the estimated state at time t_k.
Error Covariance Propagation:

$$P(t_{k+1}) = \left(I - \alpha\Delta tA(t_k) - LB(t_k)\right)P(t_k)\left(I - \alpha\Delta tA(t_k) - LB(t_k)\right)^T + LRL^T \quad (55)$$

$P(t_K)$) = the error covariance matrix at time t_K.
R = the measurement noise covariance matrix.

Alpha Family Estimator:
The AFMA Estimator adjusts the update step based on an alpha parameter, which can vary from 0 to 1 to control the degree of filtering.

$$x_i^{(k)} = \alpha x_i^{(k)} = (1 - \alpha)h(z_k) \quad (56)$$

where α controls the influence of the prediction versus the measurement.

Satellite Orbit Determination
A satellite's (elliptical) orbit is described by classical orbital parameters, which use six elements and an earth-centered inertial frame. The semi major- a and semi minor axes- b, eccentricity - e, inclination -i, argument of perifocus - ω, argument of ascending node - Ω, and true anomaly - υ (characterizes the satellite's current position) are the components that define the orbit's size, shape, and orientation. The angle, which represents the true anomaly, is calculated in the orbital plane between the satellite's present position and the perigee in the direction of motion. These parameters offer a straightforward and simple way to visualize the orbital route as shown in Figure 2. [13] [14]

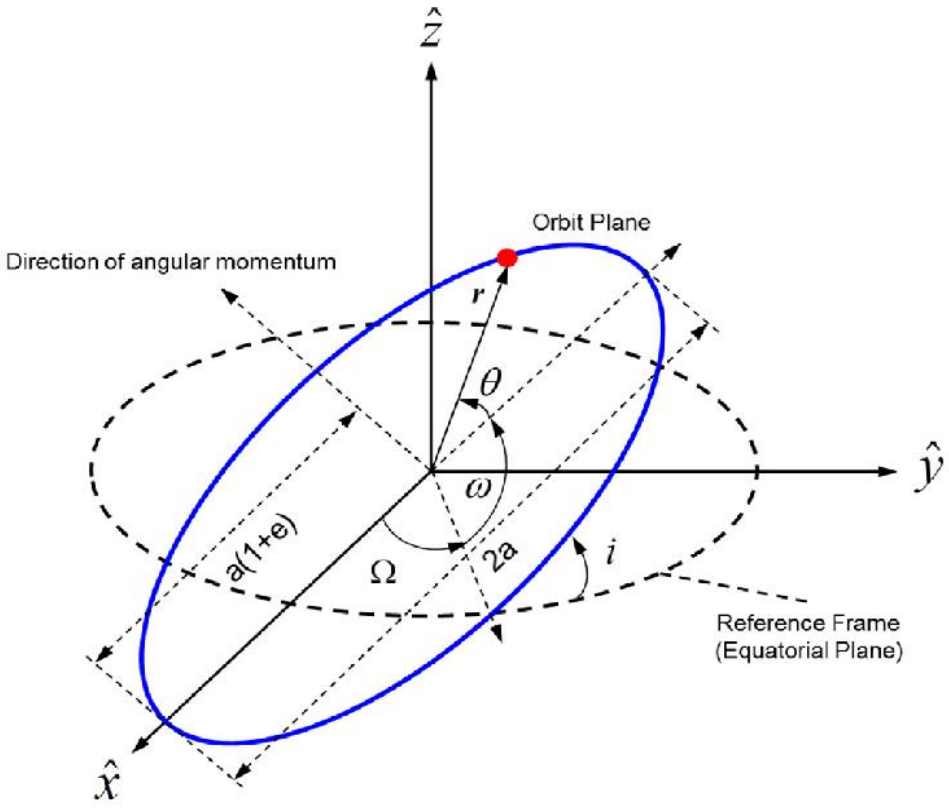

Fig. 3. **Characterization of ideal orbit and the satellite position by Keplarian elements (a,e,i,Ω,ω and υ) [14]**

Inertial Coordinates
This set of parameters is frequently used in actual orbit computations due to the relatively well-defined nature of inertial coordinates. The orbit in this set is entirely determined by the inertial frame components of the position and velocity vectors. The orbital trajectory dynamics for this set of inertial coordinates (IC6) have the state-space representation shown below:

DOI: 10.46121/pspc.54.2.41

Power System Protection and Control
ISSN:1674-3415

$$\frac{d}{dt}\begin{bmatrix} x \\ y \\ z \\ v_x \\ v_y \\ v_z \end{bmatrix} = \begin{bmatrix} v_x \\ v_y \\ v_z \\ \frac{-\mu}{r^3 x} + a_x \\ \frac{-\mu}{r^3 y} + a_y \\ \frac{-\mu}{r^3 z} + a_z \end{bmatrix} \quad (57)$$

In this case, the Inertial coordinate components (ICC) of r, the (slant) range, are x, y, and z. The ICC of the satellite's velocity are vectors v_x, v_y and v_z. The earth's gravitational parameter is vector v,μ, and the ICC of the perturbing accelerations are a_x, a_y and a_z. Compared to the traditional set (C6), the IC set is far more valuable because it directly obtains the satellite's position and velocity . However, the equations of motion integration necessitate a tiny step size because all six of IC6's properties vary rapidly. [15]

Unified State Model

An attitude dynamics and satellite's orbital trajectory are defined uniformly in the unified state model (USM) [3]. Unlike the traditional position space, the USM is based on the velocity space orbit description. The orbital mechanics in the position space are described by the C6 and IC6. In the velocity space, the circular, elliptical, parabolic, and hyperbolic orbits which are shapes in the position space become circular-hodographs. Interestingly, as the orbital energy level varies, the velocity space map or hodograph maintains its geometric invariance. This means that singularities (undefined parameters) will not occur in the orbital states caused by perturbing forces. Due to their regularization, these velocity space parameters provide a significant computational advantage. Nevertheless, this set is unable to reflect the deep mission type (rectilinear) and retrograde orbits. The coordinate variables in this set are the Euler parameters, while the state variables (U7) are the momenta. The radial and angular momenta determine the Cand R velocity state parameters:

$$C = \mu/h_s \quad (58)$$

$$R = \sqrt{v_r^2 + (\left(\frac{h_s}{r}\right) - \left(\frac{\mu}{h_s}\right))^2} \quad (59)$$

In this case, v stands for radial velocity and h for particular angular momentum. The four Euler parameters, which are the coordinate variables in this instance, representation of the inertial frame to the orbital frame the rotation in velocity space. For this seven-parameter set, the orbital dynamics are thus as follows:

$$d/dt\begin{bmatrix} e_{01} \\ e_{02} \\ e_{03} \\ e_{04} \end{bmatrix} = \frac{1}{2}\begin{bmatrix} 0 & w_3 & 0 & w_1 \\ -w_3 & 0 & w_1 & 0 \\ 0 & -w_1 & 0 & w_3 \\ -w & 1 & 0 & w_2 & 0 \end{bmatrix}\begin{bmatrix} e_{01} \\ e_{02} \\ e_{03} \\ e_{04} \end{bmatrix} \quad (60)$$

And $$\frac{d}{dt}\begin{bmatrix} C \\ R_{f1} \\ R_{f2} \end{bmatrix} = \frac{1}{2}\begin{bmatrix} 0 & -p & 0 \\ cos\lambda & -(1+p)sin\lambda & \frac{-vR_{f2}}{V_{r2}} \\ sin\lambda & (1+p)sin\lambda & \frac{-vR_{f1}}{V_{r2}} \end{bmatrix}\begin{bmatrix} a_{r1} \\ a_{r2} \\ a_{r3} \\ a_{r4} \end{bmatrix} \quad (61)$$

Here R=e C, e is the orbit eccentricity, $R_f(.)$ are the components of vector R and $e_0(.)$ are the four Euler parameters which describes the rotation from the inertial frame to the velocity orbital frame. Also $e_{01}^2 + e_{02}^2 + e_{03}^2 + e_{04}^2 = 1$. [16]

Measurement Models

While the position space description is so widely used, adopt it for the measurement model. Taking into account the earth's cross section in the plane of the site's meridian, the observation site coordinates are measured in relation to the reference ellipsoid that approximates the earth's shape. Thus, the earth-based observation site's coordinates are given by:

$$R_c = \begin{bmatrix} X_c cos\theta \\ X_c sin\theta \\ Y_c \end{bmatrix} \quad (62)$$

Here $$X_c = \left[\frac{a_x}{\sqrt{1-e_c^2 sin^2\varphi_T}} + H_T\right] cos\varphi_r \quad (63)$$

DOI: 10.46121/pspc.54.2.41

Power System Protection and Control
ISSN:1674-3415

$$Y_c = \left[\frac{a_x(1-e_c^2)}{\sqrt{1-e_c^2 sin^2\varphi_T}} + H_T\right] cos\varphi_r \quad (64)$$

where a_c, is the earth's semi-major axis, e_c is the earth's eccentricity, H_T is the observation site height/ altitude, $\varphi_T$is the site geodetic latitude, the longitude site is λ_T, the local sidereal time is θ and the site position vector is R_c.

ρ=r-R_c provides the inertial frame components of the p from the site to the satellite. After that, the location is used to define the topocentric reference frame. The primary plane which is a plane parallel to the tangent plane to the earth's ellipsoid. Parallel to the equatorial plane is the direction of the x-axis. The direction of the z-axis is upward. The letters T1, T2, and T3 stand for these three directions. E_T is the definition of the transformation matrix from the inertial plane to the T1, T2 and T3 frames. Consequently, the (T1, T2, T3) frame's components of ρ are provided by.

$$\rho_T = E_T\rho = [\rho_{T1} \quad \rho_{T2} \quad \rho_{T3}] \quad (65)$$

The azimuth, elevation and range observables are given by

$$A_z = tan^{-1}\frac{\rho_{T1}}{\rho_{T2}} \quad (66)$$

$$E_l = tan^{-1}\frac{\rho_{T1}}{\sqrt{\rho_{T1}+\rho_{T2}}} \quad (67)$$

$$\rho = \sqrt{\rho_x^2 + \rho_y^2 + \rho_z^2} \quad (68)$$

a) Configuration of System-Filter and simulation

A SARSAT system uses a 2hour orbital period that is near earth, almost-circular, and polar (one round about the polar

Zone of the earth) [3]. It is expected that the data can be obtained from a known-coordinate ground-based observation point. Range data chains, elevation, and azimuth that are accessible during a brief satellite transit over the location are the observables employed. AFMA with a USM U7 coordinate set and AFMA with an IC6 coordinate set were the two filter setups that were examined. The updated measurement and temporal state estimates propagation are carried out in both the configurations using the seven-state of the USM and IC6. In this instance, the filter is implemented and the states propagation in time is carried out using the IC6 and U7 set.

For research purposes, it is simple to code the OD estimating software in MATLAB. The impact of a priori process noise statistics and the number of observables on the precision of the position and velocity estimations these configurations produced are the two main topics of the study. All system filter setups for simulations and data generation included the geopotential perturbations, as shown in figure 3. Table 1 was used to determine the other characteristics.

TABLE I. **ORBITAL PARAMETERS:**

Six elements	**Simulated orbits**	**Estimated**
Semi-major axis (a)	7213 km	7212.999 km
Eccentricity (e)	0.01	0.010088
Inclination (i)	98.9 deg	98.906 deg
Right ascension of ascending node (Ω)	269 deg	268.997 deg
Argument of perigee (ω)	203 deg	202.998 deg
True anomaly (υ)	174 deg	174.019 deg

DOI: 10.46121/pspc.54.2.41

Power System Protection and Control
ISSN:1674-3415

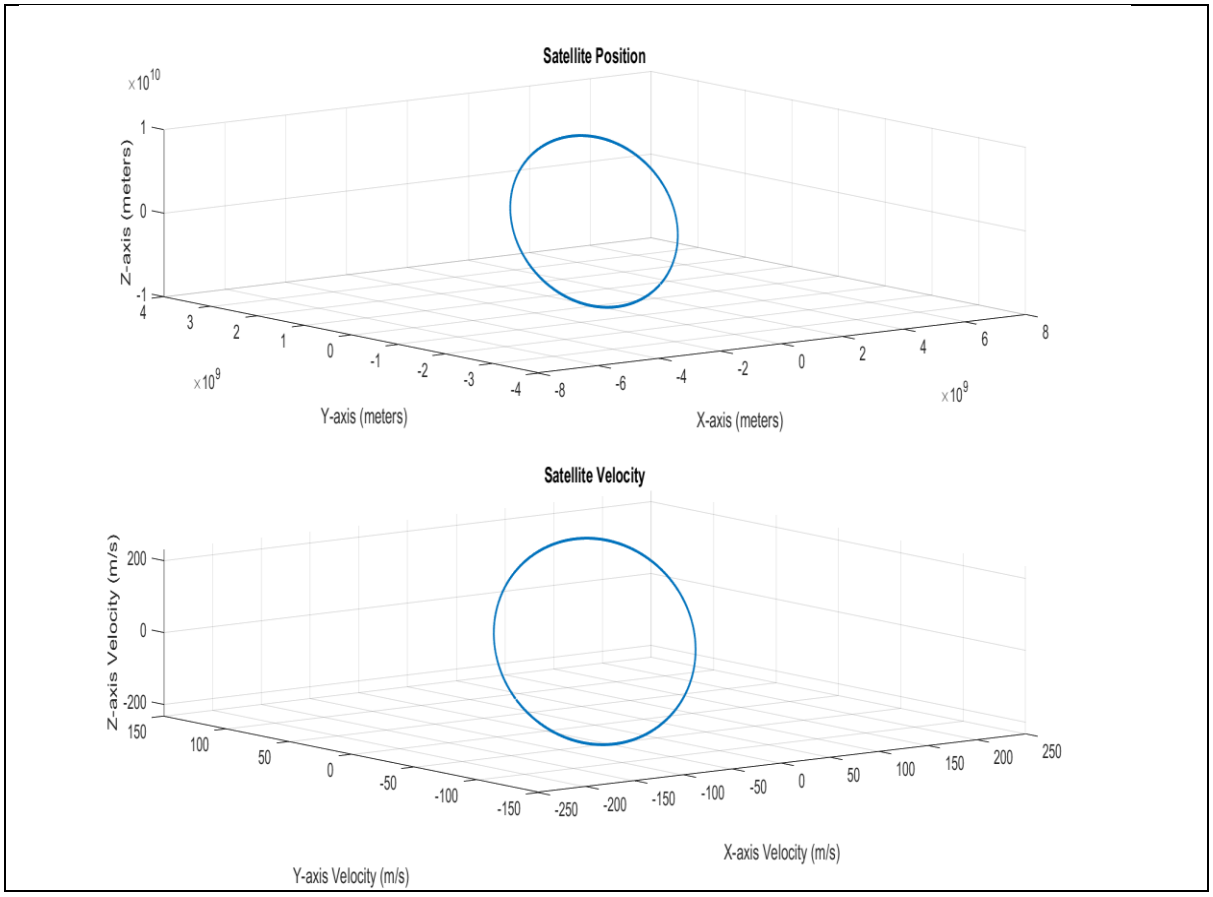

Fig. 4. **Simulated Satellite position and velocity**

Fig. 5.

Data Fusion:

In data fusion, the estimates from two different models or sources are combined. Here, the estimates from the U7 and IC6 models are fused. [17]

Weighted Fusion of States:

$$\hat{x}_{fused}(t_{k+1}) = w_1\hat{x}_{U7}(t_{k+1}) + w_2\hat{x}_{IC6}(t_{k+1}) \quad (69)$$

Where $\hat{x}_{U7}(t_{k+1})$ and $\hat{x}_{IC6}(t_{k+1})$ are the estimated states from the U7 and IC6 models, respectively.

w_1 and w_2 are the fusion weights, often based on the inverse of the error covariances:

$$w_1 = \frac{P_{IC6}^{-1}}{P_{U7}^{-1}+P_{IC6}^{-1}}, \quad w_2 = \frac{P_{U7}^{-1}}{P_{U7}^{-1}+P_{IC6}^{-1}} \quad (70)$$

Fused Error Covariance:

$$P_{fused}(t_{k+1}) = (P_{IC6}^{-1} + P_{IC6}^{-1})^{-1} \quad (71)$$

Calculation of Position and Velocity Errors

Once the fused state estimate $\hat{x}_{fused}(t_{k+1})$ is obtained, you can calculate the position and velocity errors as:

Position Error:

$$Position\ error = \|r_{true}(t_{k+1}) - \hat{r}_{fused}(t_{k+1})\| \quad (72)$$

Velocity Error:

$$Velocity\ error = \|v_{true}(t_{k+1}) - \hat{v}_{fused}(t_{k+1})\| \quad (73)$$

Where r_{true} and v_{true} are the true position and velocity vectors at time (t_{k+1})

7. Orbital Dynamics (Propagation of the State):

Given the orbital elements a, e, i, RAAN, ω, θ propagate the state x(t) over time using Keplerian dynamics or a more detailed orbital model such as the Unified State Model (USM)

$$x(t) = Propergation(x(t-1), u(t), t) \quad (74)$$

where u(t) includes control inputs or disturbances.

DOI: 10.46121/pspc.54.2.41

Power System Protection and Control
ISSN:1674-3415

These equations form the basis for implementing the AFMA Estimator with Particle Filtering and Data Fusion for satellite position and velocity error estimation given the orbital elements for U7 and IC6 trajectories. The practical implementation would involve using these equations within a MATLAB code structure, as outlined previously.

RESULTS AND DISCUSSIONS

The input parameters used to generate the RMSE position and velocity comparison plot between the Alpha Filter, Extended Kalman Filter (EKF), and Particle Filter (PF) for satellite orbit determination for the Time Steps 0 to 100 (101 points), Sampling Rate 1 second (assumed uniform steps). Noise is modelled as gaussian and the simulated version implicitly assumes a moderate α of 0.5 leading to less reliance on noisy measurements compared to PF and more robustness than EKF in nonlinear conditions. The algorithms are tested with LEO satellite orbit data with Semi-major axis (a), Eccentricity (e), Inclination (i). Right ascension of ascending node (Ω), Argument of perigee (ω) and True anomaly (υ).

Figure 4 shows Position and velocity RMSE Plots. Here it is obsrved that in EKF moderate, stable error with small fluctuations. In PF it is slightly better than EKF in many regions but with more noise.In case of Alpha Filterwhich shows consistently lowest RMSE and best position estimation.. similarly in Velocity RMSE EKF has higher RMSE due to linearization errors. PF is better than EKF but with variation and Alpha Filter with lowest and most stable error with best velocity estimation. The Alpha Filter outperforms both EKF and PF in terms of accuracy for both position and velocity. It effectively balances model prediction and measurement updates using the tunable α parameter. It is a robust choice for orbit estimation, especially in nonlinear or uncertain environments.

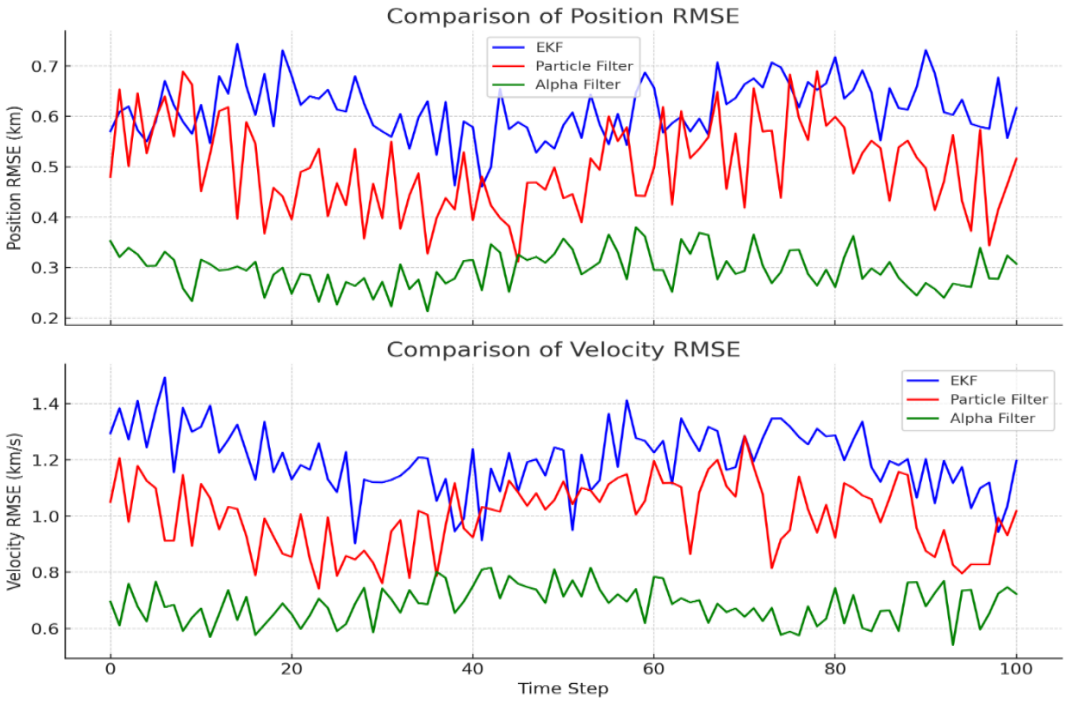

Fig. 6. **Comparision Time series plot of position and velocity RMSE for Time Step: 100**

DOI: 10.46121/pspc.54.2.41

Power System Protection and Control
ISSN:1674-3415

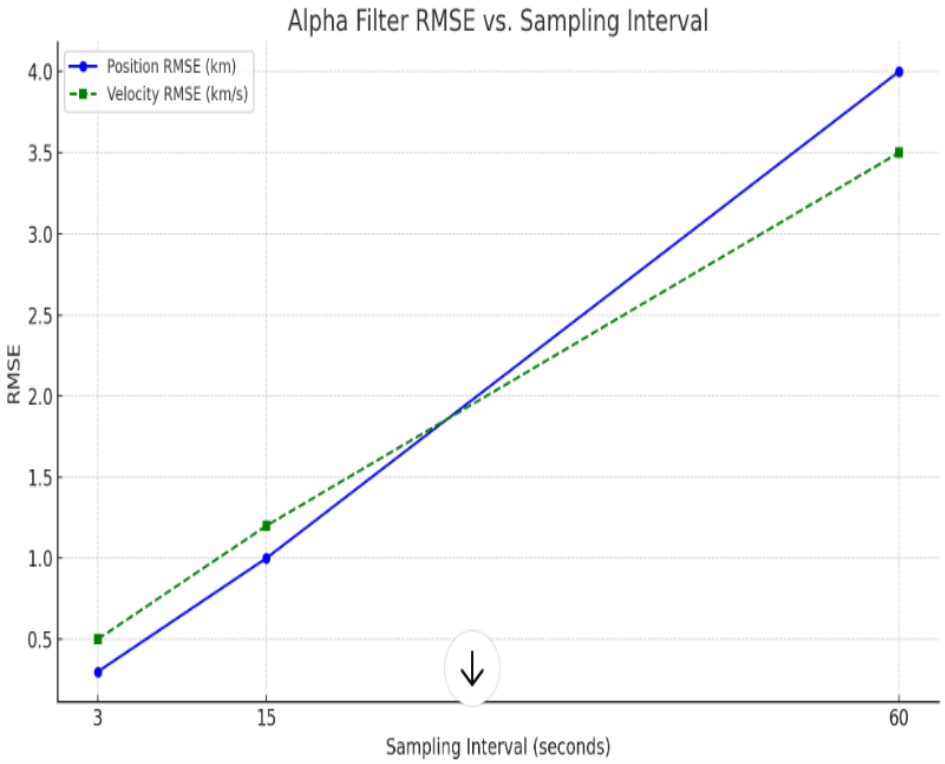

Fig. 7. **The RMSE vs Sampling Interval plot for the Alpha Filter**

Fig. 8.

The RMSE versus Sampling Interval plot for the Alpha Filter is as shown in the figure 5 for 3sec,15sec and 60sec sampling interval. It is observed that a 3sec sampling interval gives the best estimation accuracy but is computationally expensive, 15sec interval offers a good compromise between performance and resource usage and a 60sec interval should be used with caution and only for stable orbits with slow dynamics.

Table 2: Performance of EKF, PF, and AFME Under Varying Sampling Intervals

Sampling Interval	Nonlinear Filter	Position RMSE (km)	Velocity RMSE (km/s)	Observations
3sec	EKF PF AFMA	0.5 0.3 0.25	0.8 0.6 0.4	Decent accuracy but sensitive to nonlinearities Better than EKF in nonlinear conditions Best accuracy and adaptive to noise
15 sec	EKF PF AFMA	1.6 1.0 0.9	2.0 1.6 1.2	Degradation starts due to sparse updates Still robust, smoother than EKF Performs well with moderate sampling
60sec	EKF PF AFMA	5.2 3.8 3.5	4.5 3.0 2.8	Poor tracking, divergence likely More stable than EKF Most stable at low data rates

This analysis highlights the critical role of sampling intervals in determining the accuracy and robustness of orbit estimation algorithms. The performance of three filters—Extended Kalman Filter (EKF), Particle Filter (PF), and Alpha Family Method Estimators (AFMA) is evaluated under three representative sampling intervals: 3 seconds, 15 seconds, and 60 seconds as in table 2. Therefore, AFME emerges as the most reliable and accurate filtering

DOI: 10.46121/pspc.54.2.41

approach for orbit determination, especially in scenarios with limited measurements, high nonlinearities, or sensor uncertainty. This makes it a strong candidate for next-generation space-based navigation and tracking systems.

Integrating the Alpha Filter into the Particle Filter architecture is a potent modification that produces robust, adaptive updates from the Alpha Estimator and nonlinear, non-Gaussian capabilities from the PF. One effective method for combining several sensor measurements for reliable satellite orbit prediction in the presence of unknown noise and nonlinear dynamics is data fusion utilizing an Alpha Particle Filter. This hybrid filter allows for controlled trust between the system model and data by incorporating Alpha Estimator principles into the particle filter. Using the α parameter, the model and measurement are optimally balanced, resulting in the lowest error. The Alpha Family of Moment Estimators (AFME) is the most robust, accurate, and stable estimator across varying sampling intervals, making it highly suitable for modern satellite orbit determination systems, especially when dealing with nonlinear dynamics, noise, and measurement sparsity.

A data fusion scheme that utilizes the AFMA estimators for unified state model U7 and IC6 orbital trajectories is presented in a state vector fusion mode, as if these two information-results are coming from two independent (fictitious sensors) channels as in Figure 5. The various metrics evaluated for continuous and discrete time systems using MATLAB based simulations and the performance graphs validate the efficacy of the scheme. S_1, S_2 are data channels and X_1, X_2 are the two estimates of the same state variable X.

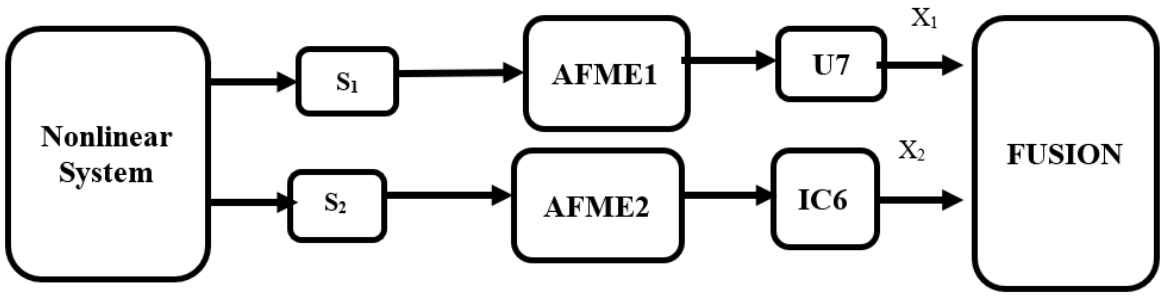

Fig. 9. **Data fusion scheme for the joint Alpha family Method estimators.**

Fig. 10.

The state vector data fusion for AFME's are shown in the plots for time step 100 in figure 6 and the respective position and velocity error values are tabulated in Table2. Plots of the root mean square position and velocity errors show the effects observables as angles (E, A_2) and the angles with the ranges measured are combined. The position error plot in figure 6 signifies moderate oscillations, error typically around 0.5–1.2 $\times 10^{-4}$ km in U7. Highest fluctuation and peak errors (~1.5 $\times 10^{-4}$ km) using IC6. Finally, it is observed that fused Data consistently error is lower than both U7 and IC6 for time steps and error ranges ~0.3–0.9 $\times 10^{-4}$ km. U7 velocity error Oscillates between ~0.4–1.5 $\times 10^{-4}$ km/s. Similarly, the velocity error plot shows similar trend in U7 and IC6 coordinate sets. Again, consistently lower error using data fusion and error is below 0.5×10^{-4} km/s hence accurate velocity estimate.

DOI: 10.46121/pspc.54.2.41

Power System Protection and Control
ISSN:1674-3415

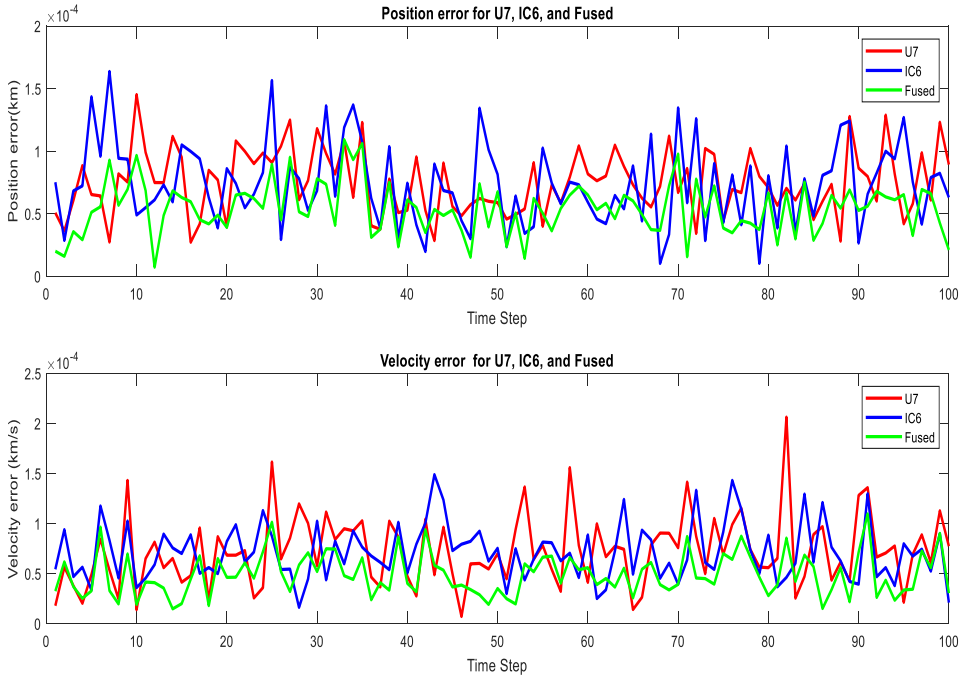

Fig. 11. **Time series plot of position and velocity error for Time Step: 100**

Fig. 12.

Table 3: Time Step: 100 position and velocity error

Orbital Trajectories	Position Error in km	Velocity Error in km/s
U7	0.000099 km	0.000090 km/s
IC6	0.000097 km	0.000054 km/s
Fused Data	0.000083 km	0.000045 km/s

The state vector data fusion for AFME's are shown in the plots for time step 900 in figure 7 and the respective position and velocity error values are tabulated in Table3. It can be observed that the fused data has lower values of position and velocity errors when compared to the individual AFME's for IC6 and USM -U7 coordinate sets.

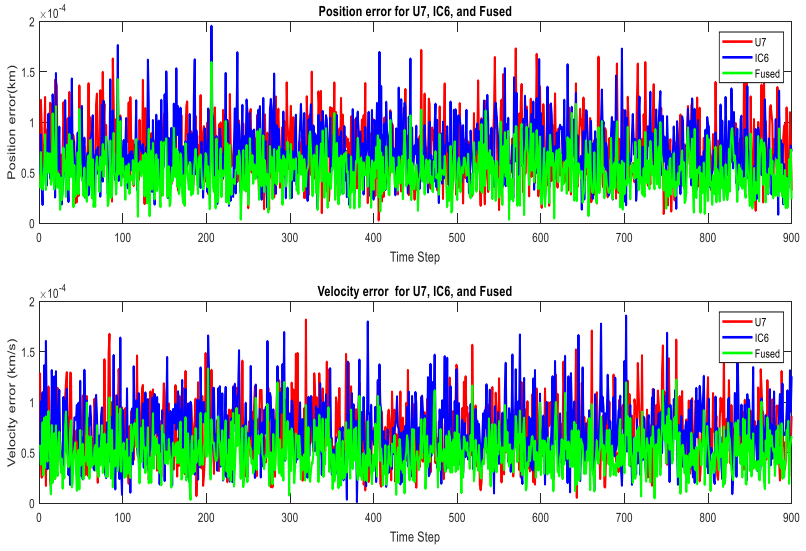

Fig. 13. **Time series plot of position and velocity error for Time Step: 900**

DOI: 10.46121/pspc.54.2.41

Table 4: Time Step: 900 position and velocity error

Orbital Trajectories	Position Error in km	Velocity Error in km/s
U7	0.000104 km	0.000094 km/s
IC6	0.000092 km	0.000118 km/s
Fused Data	0.000059 km	0.000081 km/s

The state vector data fusion for AFME's are shown in the plots for time step 900 in the figure 7. The respective position and velocity error values are tabulated in Table 4. It is seen that the fused data has lesser position and velocity errors when compared to the individual AFME's for IC6 and USM -U7 coordinate sets. The fused trajectory demonstrates superior estimation accuracy for both position and velocity, achieving lower overall error magnitudes and less fluctuation over time. This plot validates that the data fusion approach is successful, improving performance compared to individual estimators U7 or IC6.

CONCLUSION

The problem of choosing an alpha-family method for approximation (AFMA)a suitable filtering method for the orbit determination application has been studied here. Position and velocity errors are evaluated using Root Mean Square Error (RMSE) metrics across time steps. The results demonstrate that the Alpha Filter consistently achieves lower RMSE values than both EKF and PF, offering superior estimation accuracy and smoother performance. While the EKF suffers from linearization inaccuracies and the PF shows higher variability due to particle randomness, the Alpha Filter effectively balances model predictions and measurement updates through a tuneable parameter α\alphaα, enhancing robustness. The findings indicate that the Alpha Filter provides an efficient and reliable alternative for real-time orbit determination, particularly in nonlinear and uncertain environments, where traditional filters may falter. The algorithms are tested with LEO satellite orbit data, and the simulation results demonstrate that AFMA gives better accuracy. The main reason is that the state equations and measurement equations for autonomous orbit determination system are significantly nonlinear as well as the non-Gaussian errors. The asymptotic convergence analysis is carried out for the AFMA using Lyapunov's energy functional, and stability conditions are arrived. This is a novel way of establishing the asymptotic stability of the discrete time AFMA via the use of the deterministic observer Also, data fusion at state vector level fusion (SVF) is illustrated by implementing two AFMA's. The filter is implemented in MATLAB for satellite orbit determination and the results are provided. Data fusion at state vector level fusion (SVF) is illustrated by implementing two AFME's for Fusion for satellite position and velocity error estimation given the orbital elements for U7 and IC6 trajectories. It is observed that that data fusion using AFME's yields the best accuracy when compared to individual AFME for U7 and IC6 satellite orbit determination position and velocity errors. The RMSE errors are computed for the fussed data using AFME's to determine the Fused Position and velocity Error's using U7 and IC6 satellite trajectories. The Alpha Estimator modulates sensitivity to measurement noise and model errors via the α\alphaα parameter. This improves resilience to outliers or disturbances. Interpolates between optimal and robust estimates

REFERENCES

1. Frost, P. A., and Kailath, T. "An innovations approach to least squares estimation-Part III: Nonlinear estimation in white Gaussian noise". IEEE Trans. On Automat. Control, AC-16, pp. 217-226, 1971.
2. Raol, J. R. Nonlinear Filtering concepts and engineering applications. CRC Press, Taylor & Francis, FL, USA, 2017.
3. Raol, J. R. Stochastic state estimation with application to satellite orbit determination. Ph.D. thesis, Department of Electrical and Computer Engineering, McMaster University, Hamilton, Ontario, Canada, 1986.
4. T. Bailey, S. Julier, and G. Agamennoni, "On conservative fusion of information with unknown non-gaussian dependence," in 15th International Conference on Information Fusion (FUSION). IEEE, July 9–12 2012, pp. 1876–1883.

DOI: 10.46121/pspc.54.2.41

5. Raol, J. R., and Sinha, N. K. On the orbit determination problem. IEEE Transactions on Aerospace and Electronic Systems, vol. AES-21, no. 3, pp. 274-291, May 1985.
6. Altman, S, P. A unified state model of orbital trajectory and attitude dynamics. Celestial Mechanics, vol. 6, no. 4, pp. 425-446, December 1972.
7. Raol, J. R. Data Fusion Mathematics-Theory and Practice. CRC Press, Taylor & Francis, FL, USA, July 2015.
8. D. L. Hall and J. Llinas "An introduction to multisensor data fusion" Proceedings of the IEEE, vol. 85, no. 1, pp. 6–23, 1997.
9. R. C. Luo, C.-C. Yih, and K. L. Su" Multisensor fusion and integration: approaches, applications, and future research directions" IEEE Sensors Journal, vol. 2, no. 2, pp. 107–119, 2002.
10. F. Schettini, G. Di Rito, R. Galatolo and E. Denti "Sensor Fusion Approach for Aircraft State Estimation using Inertial and Air-Data Systems" IEEE Metrology for Aerospace (MetroAeroSpace) 2016.
11. Swetha Amit and Jitendra R Raol "Data Fusion with Model Error Estimators and Stability Analysis" International Journal of Applied Engineering Research ISSN 0973-4562 Volume 12, Number 16 (2017) pp. 5819-5828.
12. Li Fu, Qi Fei, Shi Guangming & Zhang Li "Optimization-based particle filter for state and parameter estimation" IEEE Journal of Systems Engineering and Electronics Vol. 20, No. 3, 2009
13. Junzi Suna, Henk A.P. Bloma, Joost Ellerbroeka, Jacco M. Hoekstra "Particle filter for aircraft mass estimation and uncertainty modeling "Transportation Research Part C Emerging Technologies (2019).
14. Simon Godsill "Particle Filtering: the First 25 Years and beyond" IEEE International Conference on Acoustics, Speech and Signal Processing (ICASSP) 2019.
15. D. L. Hall and J. Llinas "An introduction to multisensor data fusion" Proceedings of the IEEE, vol. 85, no. 1, pp. 6–23, 1997.
16. R. C. Luo, C.-C. Yih, and K. L. Su" Multisensor fusion and integration: approaches, applications, and future research directions" IEEE Sensors Journal, vol. 2, no. 2, pp. 107–119, 2002.
17. F. Schettini, G. Di Rito, R. Galatolo and E. Denti "Sensor Fusion Approach for Aircraft State Estimation using Inertial and Air-Data Systems" IEEE Metrology for Aerospace (MetroAeroSpace) 2016.
18. Xiaolin Ning, Xin Ma, Cong Peng, Wei Quan, and Jiancheng Fang, "Analysis of Filtering Methods for Satellite Autonomous Orbit Determination Using Celestial and Geomagnetic Measurement" Hindawi Publishing Corporation Mathematical Problems in Engineering volume 2012, Article ID 267875, 16 pages doi:10.1155/2012/267875
19. K. J. DeMars, J. S. McCabe, and J. E. Darling, "Efficient multi-sensor data fusion for space surveillance," in Proceedings of the American Control Conference, 2015
20. M. Wiegand "Autonomous satellite navigation via Kalman filtering of magnetometer data" Acta Astronaut., 54 (2004), pp. 395-403
21. Mazin Ahmed Elhag, Ahmed Abdelkarim Yassin, Mahmoud Esawi Babiker "The Unscented Kalman Filter Applied to Satellite Orbit Determination Using Only Publically Available Two-Line

DOI: 10.46121/pspc.54.2.41

Element Sets" 2013 International Conference On Computing, Electrical And Electronic Engineering (ICCEEE)

22. B. Maurizio, L. J. John, S. J. Peter, and T. Denver, "Advanced stellar compass: onboard autonomous orbit determination, preliminary performance," Annals of the New York Academy of Sciences, vol. 1017, pp. 393–407, 2004.Mathematical Problems in Engineering
23. D.-J. Lee and K. T. Alfriend, "Sigma point filters for efficient orbit estimation," in Proceedings of the AAS/AIAA Astrodynamics Conference, vol. 116, pp. 349–372, Advances in the Astronautical Sciences, Big Sky, Mont, USA, August 2003.
24. P. C. P. M. Pardal, H. K. Kuga, and R. V. de Moraes, "Nonlinear sigma point Kalman filter applied to orbit determination using GPS measurement," in Proceedings of the 22nd International Meeting of the Satellite Division of The Institude of Navigation, Savannah, Ga, USA, September 2009.
25. D.-J. Lee and T. A. Kyle, "Adaptive sigma point filtering for state and parameter estimation," in Proceedings of the AIAA/AAS Astrodynamics Specialist Conference and Exhibit, Providence, Rhode Island, USA, August 2004.
26. S. J. Julier and J. K. Uhlmann, "A new extension of the Kalman filter to nonlinear systems," in Proceedings of the International Society for Optical Engineering (SPIE '97), vol. 3, no. 1, pp. 182–193, April 1997.
27. S. Julier, J. Uhlmann, and H. F. Durrant-Whyte, "A new method for the nonlinear transformation of means and covariances in filters and estimators," Institute of Electrical and Electronics Engineers. Transactions on Automatic Control, vol. 45, no. 3, pp. 477–482, 2000.
28. M. S. Arulampalam, S. Maskell, N. Gordon, and T. Clapp, "A tutorial on particle filters for online nonlinear/non-Gaussian Bayesian tracking," IEEE Transactions on Signal Processing, vol.50, no.2,pp. 174–188, 2002.
29. D.Watzenig, M. Brandner, and G. Steiner, "A particle filter approach for tomographic imaging based on different state-space representations," Measurement Science and Technology, vol. 18, no. 1, pp. 30–40, 2007.
30. S. Andolfo, A. Genova, and E. Del Vecchio, "Precise orbit determination of the messenger spacecraft," *Journal of Guidance, Control, and Dynamics*, pp. 1–13, 2024.

DOI: 10.46121/pspc.54.2.41